

# Naphthalene-based water-soluble fluorescent boronic acid isomers suitable for ratiometric and off-on sensing of saccharides at physiological pH<sup>†</sup>

Xingming Gao, Yanling Zhang and Binghe Wang\*

Department of Chemistry and Center for Biotechnology and Drug Design, Georgia State University, PO Box 4098, Atlanta, GA 30302-4098, USA. E-mail: wang@gsu.edu; Fax: +1 404 654 5827; Tel: +1 404 651 0289

Received (in St. Louis, MO, USA) 31st August 2004, Accepted 6th December 2004  
First published as an Advance Article on the web 28th February 2005

Two water-soluble naphthalene-based fluorescent boronic acid isomers, 5-(dimethylamino)naphthalene-1-boronic acid (5-DMANBA, **1**) and 4-(dimethylamino)naphthalene-1-boronic acid (4-DMANBA, **2**), have been synthesized; their fluorescent properties upon binding with carbohydrates have been determined in aqueous phosphate buffer at pH 7.4. The difference in substitution pattern between **1** and **2** leads to significant differences in their fluorescence properties. For example, addition of fructose (50 mM) to a solution of **1** induced a 61% fluorescence intensity decrease at 513 nm and a 36-fold increase at 433 nm. This revealed that compound **1** is a potential sensor for *ratiometric* sensing of sugars. The pH titration curves of **1** in the absence and the presence of fructose (50 mM) showed a 93- and 200-fold fluorescence intensity increase at 433 nm, respectively, when pH was increased from 3 to 10. Compound **2**, however, does not show ratiometric fluorescent intensity changes, but shows significant fluorescence intensity increase upon addition of a sugar (41-fold intensity increase with 50 mM fructose). The emission intensity of **2** increased by over 170-fold at 445 nm upon changing the pH from 2 to 11.

## Introduction

During the last decade, a great deal of effort has been directed towards the detection of saccharides by fluorescent chemosensors.<sup>1</sup> Such sensors have been primarily developed as a way to determine analyte concentrations in solution. Most sensors contain boronic acid as the key recognition moiety,<sup>2</sup> due to its ability to form tight and reversible complexes with the diol moiety of saccharides in aqueous media.<sup>3</sup> The most common observed interactions are with *cis*-1,2- or 1,3-diols to form five- or six-membered rings, respectively.

Recently our group has demonstrated, for the first time, that boronic acid based saccharide sensors can be used for the recognition of mammalian cell surface saccharide biomarkers.<sup>4</sup> Because saccharide biomarkers<sup>5</sup> are implicated in various physiological and pathological processes, including viral and bacterial infection,<sup>6</sup> such sensors have a wide variety of potential applications in the diagnosis, detection and therapeutic intervention of human diseases.<sup>7</sup> Due to their similarity to the function of lectins,<sup>8</sup> we refer to those boronic acid based small molecules, capable of recognizing cell-surface saccharides, as boronolectins.<sup>9</sup>

The synthesis of fluorescent sensors for cell-surface saccharide recognition requires the use of fluorescent reporter compounds that change their fluorescence properties upon binding. There has been some very good early successes in this area:<sup>2</sup> for example, we have synthesized a series of fluorescent boronic acid based saccharide sensors<sup>4</sup> using an anthracene-based fluorescent reporter system developed by the Shinkai group.<sup>2b</sup> For our continuing work in developing fluorescent boronolec-

tins, we require boronic acids that (1) show significant fluorescence property changes and (2) have sufficiently high water solubility. Therefore, we have undertaken a major effort in developing water-soluble fluorescent boronic acids that change their fluorescence properties upon binding with saccharides.<sup>10</sup> In this endeavor, we are especially interested in fluorescent reporter compounds that change fluorescence intensities at more than one wavelength for ratiometric sensing.

Herein, we describe the synthesis and study of two fluorescent boronic acid isomers: 5-(dimethylamino)naphthalene-1-boronic acid (5-DMANBA, **1**) and 4-(dimethylamino)naphthalene-1-boronic acid (4-DMANBA, **2**), presented in Fig. 1. How a change in substitution pattern can dramatically influence the fluorescence behavior of such compounds will be demonstrated and discussed.

## Results and discussion

### Synthesis

4-(Dimethylamino)naphthalene-1-boronic acid (**2**) was synthesized and characterized as described in a previous communication.<sup>11</sup> The synthesis of 5-(dimethylamino)naphthalene-1-boronic acid (**1**) is depicted in Scheme 1. Starting from the readily available 1-nitronaphthalene (**3**), the intermediate, 5-nitro-1-bromonaphthalene (**4**), was synthesized by following related literature procedures.<sup>12</sup> Compound **5** was obtained by reduction of **4** with Fe/HCl in a mixture of EtOH, AcOH, dioxane and H<sub>2</sub>O (2:2:2:1) at 80 °C.<sup>12b</sup> Reaction of **5** with MeI in the presence of NaH in THF at 60 °C gave 5-(dimethylamino)-1-bromonaphthalene (**6**). **1** was synthesized from **6** through lithiation and reaction with trimethylborate. Purification of the crude product by silica gel chromatography afforded **1** as a white powder.

<sup>†</sup> Electronic supplementary information (ESI) available: <sup>1</sup>H and <sup>13</sup>C NMR spectra of compounds **1**, **4**, **5**, and **6**. See <http://www.rsc.org/suppdata/nj/b4/b413376e/>

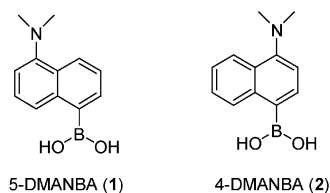


**Fig. 1** Structures of the two dimethylaminonaphthalene boronic acid isomers.

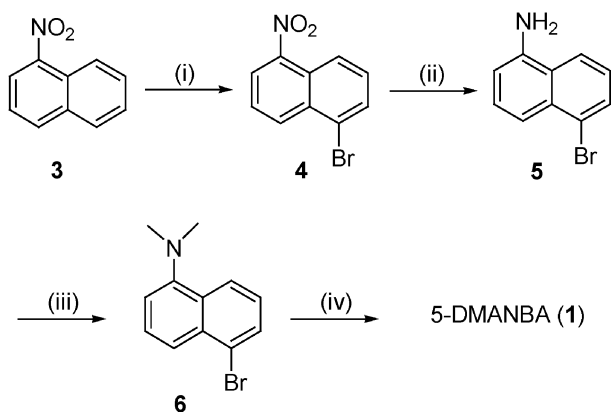
### Solubility

Because improving the water solubility is essential to this study, the solubility of the two sensors in 0.1 M aqueous phosphate buffer (pH 7.4) was determined by measuring the UV absorbance with the aid of a standard curve. **1** has a solubility of 1.2 mM ( $0.26 \text{ mg ml}^{-1}$ ) and **2** has a solubility of 0.8 mM ( $0.17 \text{ mg ml}^{-1}$ ). These millimolar concentrations will represent a high enough solubility for biological evaluations in an aqueous environment, which are often conducted at low micromolar concentrations (see below). This is especially relevant to our effort in making fluorescent boronolelectins that recognize cell-surface carbohydrate biomarkers.<sup>4</sup>

### Fluorescence properties of the sensor compounds

**Fluorescence properties of 5-DMANBA (1).** Sensor **1** exhibits an emission maximum at 513 nm [Fig. 2 and Fig. 3(A)] and an absorption maximum at 300 nm [Fig. 3(B)] in 0.1 M aqueous phosphate buffer at pH 7.4, with a Stokes shift of over 200 nm. Addition of a carbohydrate results in a significant decrease in fluorescence intensity at 513 nm, combined with a more dramatic increase at 433 nm. For example, addition of fructose (50 mM) to the solution of **1** induced a 36-fold fluorescence intensity increase at 433 nm and a 61% fluorescence intensity decrease at 513 nm (Fig. 2). An isosbestic point was observed at 495 nm. To the best of our knowledge, such large emission intensity changes at two wavelengths have never been reported for boronic acid based saccharide sensors. The quantum yield ( $\phi_F$ ) of **1** was determined to be *ca.* 0.07 at 513 nm in 0.1 M phosphate buffer (pH 7.4), in the absence of a sugar, and *ca.* 0.23 at 433 nm under the same conditions, in the presence of 50 mM of fructose [using 8-quinoline boronic acid ( $\phi_F = 0.58$  in 12 M  $\text{H}_2\text{SO}_4$ ) as a reference compound].<sup>13</sup>

To establish the general applicability of this fluorescent reporter compound **1**, we have also studied the effect of four other carbohydrates on the fluorescence intensity (Figs. 4 and 5): sorbitol, tagatose, galactose and glucose. Data at the monitoring wavelengths of 433 and 513 nm, as well as association constants  $K_a$ , are summarized in Table 1.



**Scheme 1** Synthesis of 5-DMANBA **1** (yields in parentheses): (i)  $\text{Br}_2$ ,  $\text{FeCl}_3$ , (50%); (ii)  $\text{Fe}$ ,  $\text{HCl}$ ,  $80^\circ\text{C}$  (97%); (iii)  $\text{CH}_3\text{I}$ ,  $\text{NaH}$ ,  $60^\circ\text{C}$  (85%); (iv)  $n\text{-BuLi}$ ,  $(\text{MeO})_3\text{B}$ ,  $\text{HCl}$ , (65%).

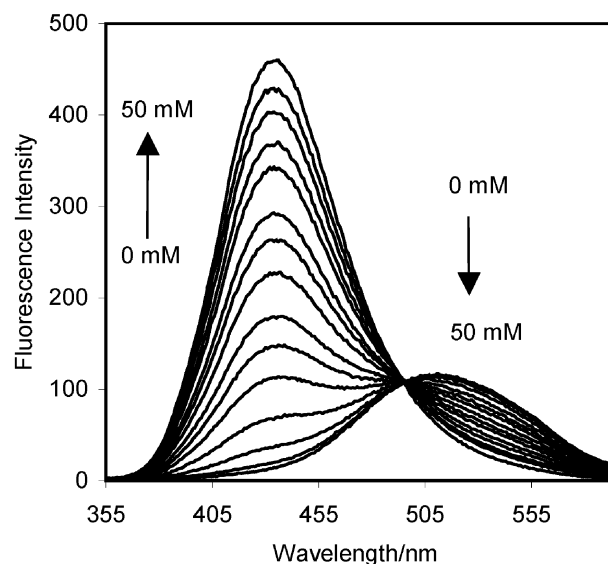


**Fig. 2** Fluorescence spectral changes of 5-DMANBA (**1**,  $1.0 \times 10^{-5}$  M) at different concentrations of D-fructose (0–50 mM) in 0.1 M aqueous phosphate buffer at pH 7.4;  $\lambda_{\text{ex}} = 300$  nm.

From Fig. 4, it is clear that all five carbohydrates tested caused very large fluorescence intensity increases at 433 nm in aqueous solution at physiological pH with varying maximal magnitudes: addition of sorbitol induced the largest fluorescence intensity increase (42-fold) at a concentration of 200

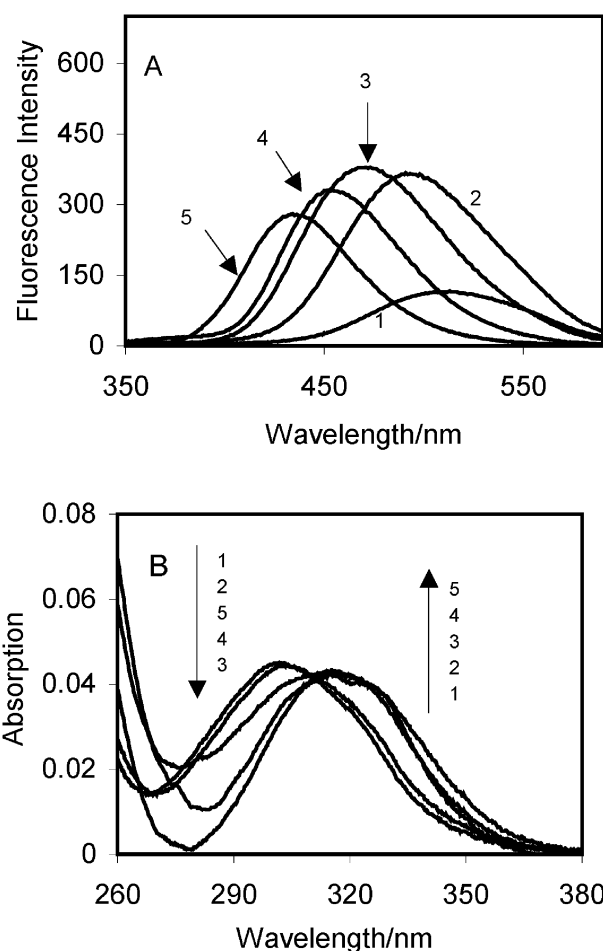


**Fig. 3** Emission (A) and absorption (B) spectra of 5-DMANBA (**1**,  $1.0 \times 10^{-5}$  M) in 0.1 M aqueous phosphate buffer at pH 7.4, in various solvents: (curve 1) buffer; (curve 2) MeOH–buffer (1 : 1, v/v); (curve 3) MeOH; (curve 4) EtOAc; (curve 5) hexanes.

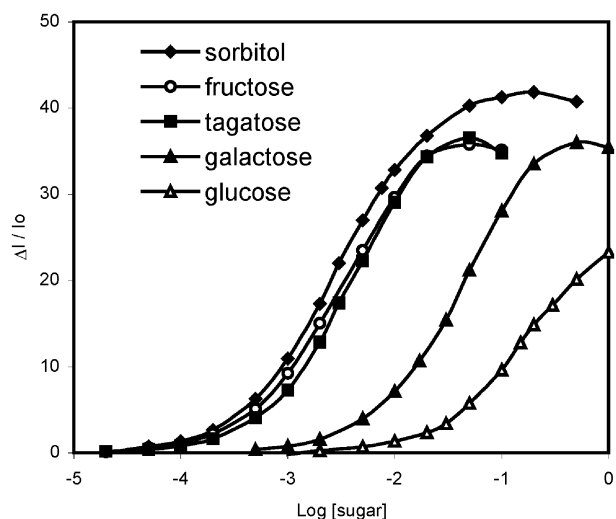


**Fig. 4** Fluorescence intensity changes ( $\Delta I/I_0$ ) of **1** ( $1.0 \times 10^{-5}$  M) as a function of sugar concentration in 0.1 M aqueous phosphate buffer at pH 7.4;  $\lambda_{\text{ex}} = 300$  nm,  $\lambda_{\text{em}} = 433$  nm.

mM; fructose, galactose and tagatose induced about 36-fold increases in fluorescence intensity; glucose, on the other hand, induced a maximum 23-fold fluorescence intensity increase at a much higher concentration (1 M).

Fig. 5 shows the effect of five carbohydrates on the fluorescence intensity of **1** at 513 nm. It is clear that all five carbohydrates tested caused a fluorescence intensity decrease (at 513 nm in aqueous solution at physiological pH) with varying magnitudes ranging from 50% to 60% at different concentrations.

Because the significant fluorescence intensity variations observed at the two wavelengths, 433 and 513 nm, are in opposite directions, large changes in the emission intensity ratios  $I_{433}/I_{513}$  were observed upon addition of the sugars to the solutions of **1** (Fig. 6). For example, the initial ratio of fluorescence intensities of 0.1:1 before addition of sugar became 8.4:1 after addition of 50 mM fructose, which represents a 84-fold change. Detectable fluorescence intensity ratio changes can be observed upon addition of low concentrations of fructose. For example, the emission intensity ratio  $I_{433}/I_{513}$  changed from 0.11 to 0.23 upon addition of only 0.1 mM of fructose. The other carbohydrates tested also exhibited large changes of this ratio at different concentrations.

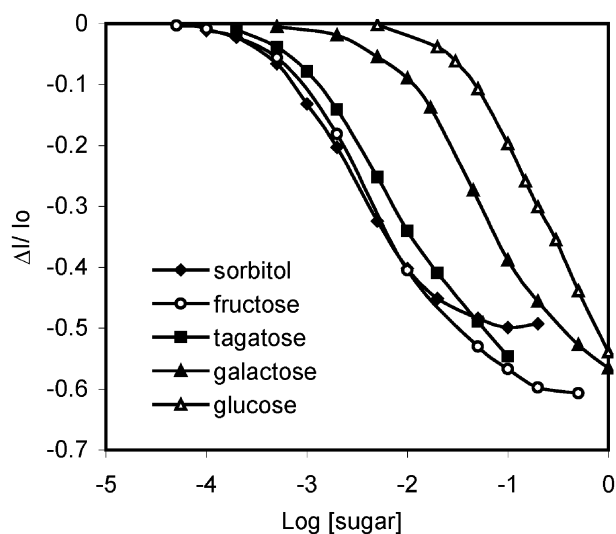


**Fig. 5** Fluorescence intensity changes ( $\Delta I/I_0$ ) of **1** ( $1.0 \times 10^{-5}$  M) as a function of sugar concentration in 0.1 M aqueous phosphate buffer at pH 7.4;  $\lambda_{\text{ex}} = 300$  nm,  $\lambda_{\text{em}} = 513$  nm.

**Table 1** Association constants ( $K_a$ ) and maximal fluorescence intensity changes ( $\Delta I/I_0$ ) of **1** at 433 and 513 nm with different sugars

Sugar	$K_a/M^{-1}$	$\Delta I/I_0$ (sugar concentration/M)	
		433 nm	513 nm
Sorbitol	$337 \pm 5$	42 (0.20)	-0.48 (0.05)
Fructose	$311 \pm 4$	36 (0.05)	-0.61 (0.05)
Tagatose	$229 \pm 3$	37 (0.05)	-0.55 (0.05)
Galactose	$23.0 \pm 0.2$	36 (0.50)	-0.56 (0.50)
Glucose	$3.6 \pm 0.1$	23 (1.0)	-0.54 (1.0)

To examine the binding more quantitatively, the association constants  $K_a$  between **1** and the five carbohydrates were determined, assuming the formation of a 1:1 complex.<sup>14</sup> As expected, the affinity trend of **1** followed that of simple monoboronic acids in the order sorbitol > fructose > tagatose > galactose > glucose (see Table 1). Indeed, these binding constants are similar to those observed with phenylboronic acid.<sup>3c</sup>

To understand the structural features associated with the fluorescence intensity changes, we studied the pH profiles of the fluorescence intensity in the absence and in the presence of fructose or glucose at a fixed concentration of 50 mM (Figs. 7–10). A strong fluorescence peak at 335 nm and a weak fluorescence peak at 513 nm were observed at low pH (1.78) in the absence of a sugar (Fig. 7). The fluorescence intensity at 335 nm decreased very quickly when pH increased from 1.78 to 7.04, and did not show further changes beyond pH 7. The fluorescence intensity at 513 nm increased very quickly when pH increased from 1.78 to 7.04, and then decreased in the pH range 7.04–10.54. Almost no fluorescence was observed at 433 nm in the pH range 1.78–7.04, while a new peak increased very significantly at 433 nm as the pH increased to 10.54.

The pH-induced spectral changes at 335 nm, in the absence of a sugar, are similar to those in the presence of 50 mM fructose or glucose (Fig. 8). A more than 30-fold intensity decrease at 335 nm was observed when pH increased from 1.78 to 7.04. Plotting the intensity changes at 335 nm against pH reveals a first apparent  $pK_a$  of 5.1 for **1** in the absence of sugar and in the presence of glucose, and 5.8 in the presence of fructose.

The pH profiles of the fluorescence intensity of **1** at 433 nm reveal the second apparent  $pK_a$  of **1**, being  $\sim 9.0$  in the absence of sugar, 6.2 in the presence of fructose, and 8.2 in the presence of glucose (Fig. 9). It is reasonable to assign the first  $pK_a$  to the

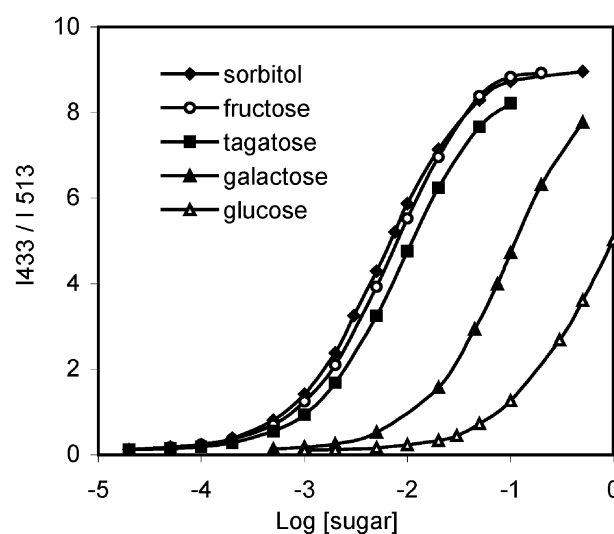


**Fig. 6** Changes of the fluorescence intensity ratio  $I_{433}/I_{513}$  of **1** ( $1.0 \times 10^{-5}$  M) as a function of sugar concentration in 0.1 M aqueous phosphate buffer at pH 7.4;  $\lambda_{\text{ex}} = 300$  nm.

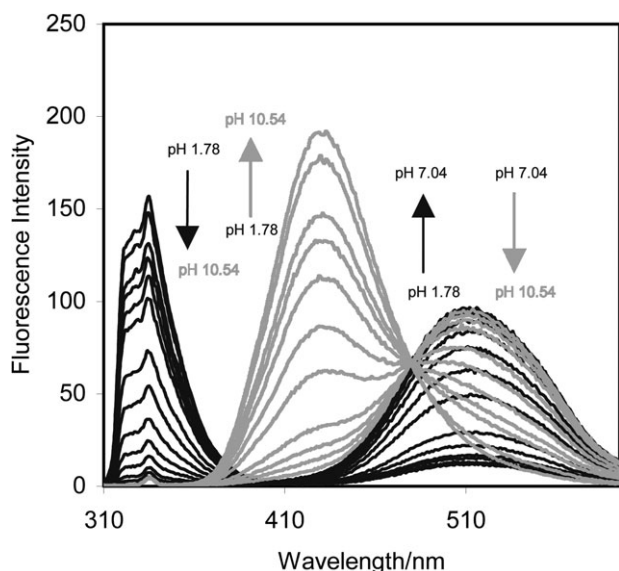


**Fig. 7** Fluorescence spectral changes of **1** ( $1.0 \times 10^{-5}$  M) in the absence of a sugar at different pH in 0.1 M aqueous phosphate buffer,  $\lambda_{\text{ex}} = 300$  nm; pH range: 1.78–7.04, blue curves; 7.04–10.54, black curves.

aniline group and the second  $pK_a$  to the boronic acid. Therefore, one can use Scheme 2 to show the various ionization states of **1**, which helps to understand the assignment of each fluorescent peak to a particular species.

At low pH (1.78), the strongest fluorescent peak is the one at 335 nm. This corresponds to the protonated aniline species with the boronic acid in a neutral trigonal state (**1a**, Scheme 2). As the pH increases, the peak intensity at 335 nm decreases with a concomitant increase for the peak at 513 nm. This change correlates with the appearance of the neutral species **1**, which has a deprotonated aniline group and a neutral trigonal boronic acid. With further increase in pH, the boronic acid begins a transition to its corresponding anionic tetrahedral species (**1b**). The disappearance of **1** correlates with a decrease in fluorescence intensity at 513 nm and an increase at 433 nm. These results indicate that it is the anionic tetrahedral boronic acid species **1b** that is responsible for the 433 nm emission. The situation is similar to the addition of a sugar, except that the transition to the anionic tetrahedral boron species occurs at a lower pH (below pH 7.4) in the presence of a sugar, due to the lowered  $pK_a$  of the sugar-boronic acid complex (see below).<sup>3c,d</sup> Therefore, at neutral pH, the observed fluorescence changes

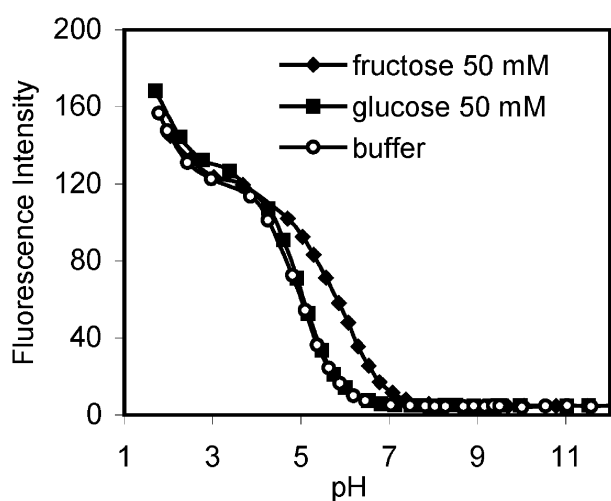


**Fig. 8** pH-dependent fluorescence intensity changes of **1** ( $1.0 \times 10^{-5}$  M) at 335 nm in the absence and in the presence of sugar in 0.1 M aqueous phosphate buffer,  $\lambda_{\text{ex}} = 300$  nm.

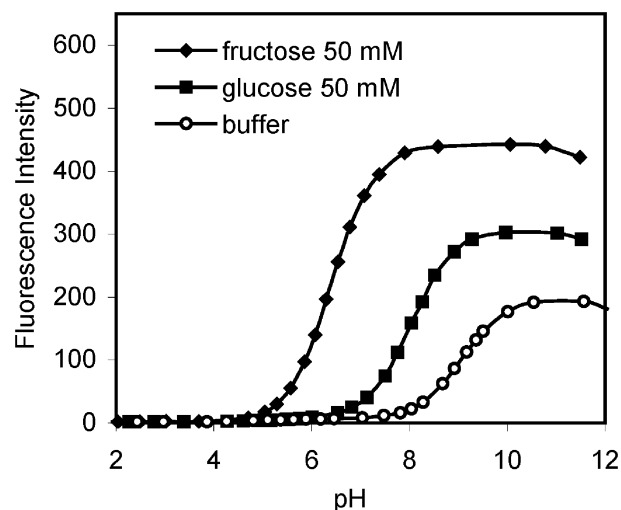
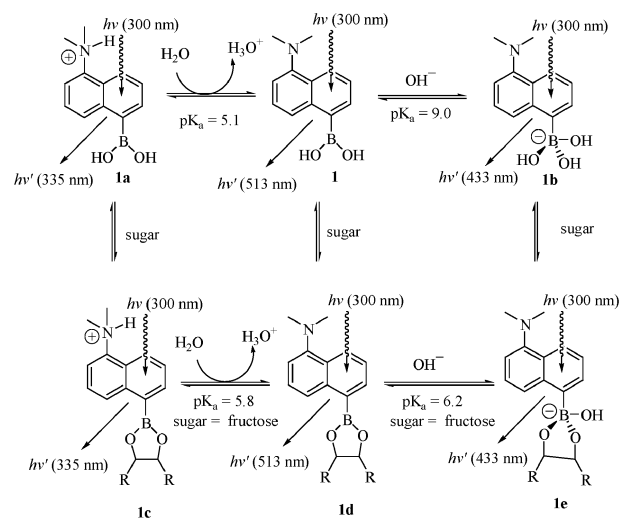


**Fig. 9** pH-dependent fluorescence intensity changes of **1** ( $1.0 \times 10^{-5}$  M) at 433 nm in the absence and in the presence of sugar in 0.1 M aqueous phosphate buffer,  $\lambda_{\text{ex}} = 300$  nm.

with the addition of a sugar are due to the conversion of **1** to **1e**.

Such an analysis is consistent with the bell-shaped curves of the pH titration profiles at 513 nm (Fig. 10), since the neutral species **1** and **1d**, which are responsible for the 513 nm emission, only exist in a certain pH range, between the two apparent  $pK_a$  values. The scenario presented in Scheme 2 is also consistent with the differences observed between the different carbohydrates. It is well-known that the binding of a carbohydrate to a boronic acid often lowers its apparent  $pK_a$ ; the extent to which the  $pK_a$  is lowered depends on the carbohydrate used.<sup>3c,d</sup> For example, the apparent  $pK_a$  of the fructose complex with phenylboronic acid is 4.5, whereas the apparent  $pK_a$  of the glucose complex is about 6.8. In contrast, the  $pK_a$  of phenylboronic acid is about 8.8.<sup>3c,d</sup> Therefore, it is reasonable to observe a shift of the pH profile curves from lower to higher pH when going from the fructose complex, to the glucose complex, to the free boronic acid **1** (Fig. 9). For the profile at 513 nm, one can see that the maximal intensity observed for the fructose complex was much lower than that of free **1** and its glucose complex (Fig. 10). This is understandable when considering the small difference between the  $pK_a$  values of the aniline amine (5.8) and the boron (6.2) in the fructose complex. This narrow range results in a quick transi-



**Scheme 2** Fluorescence properties of **1** in different ionization states, in the absence and in the presence of a sugar in 0.1 M aqueous phosphate buffer.

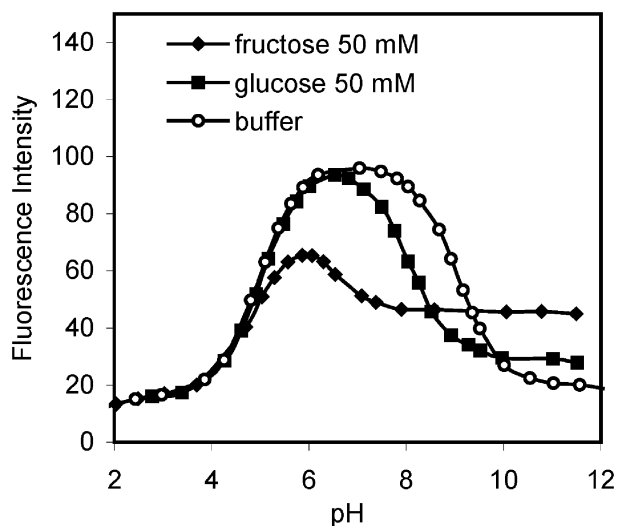


**Fig. 10** pH-dependent fluorescence intensity changes of **1** ( $1.0 \times 10^{-5}$  M) at 513 nm in the absence and in the presence of sugar in 0.1 M aqueous phosphate buffer,  $\lambda_{\text{ex}} = 300$  nm.

tion from **1c** to **1e** without a significant increase in concentration of the neutral species **1d**, seen with the sensor alone or with its glucose complex.

It should be noted that the fluorescence intensity of **1e** at 433 nm (Fig. 9) seems to be much stronger than that of **1b**, although they are both in the same ionization state. For example, the pH titration curves of **1** in the absence of a sugar showed a 93-fold fluorescence intensity increase at 433 nm when the pH increased from 3 to 10. In contrast, the fluorescence intensity of **1** in the presence of 50 mM fructose and glucose showed 200- and 150-fold increases at 433 nm, respectively, within the same pH range. Such results indicate that it is more than the ionization state changes that cause the fluorescence intensity changes. The binding itself also causes structural changes that influence fluorescence intensity. However, the exact mechanism through which such changes occur needs to be probed further, which is beyond the scope of this paper.

The study of solvent effects on the emission and absorption spectra of **1** was carried out to gain further understanding of the mechanism of the ratiometric fluorescence changes observed for **1**. A large blue shift (80 nm) was observed in the emission spectra of compound **1** when the solvent polarity was decreased [513 nm in 0.1 M aqueous phosphate buffer at pH 7.4 *versus* 433 nm in hexanes; see Fig. 3(A) above]. However, the wavelength changes in the absorption spectra were much smaller in comparison [Fig. 3(B)]. For example, the absorption maximum changed from 300 nm in aqueous phosphate buffer to 315 nm in hexanes. These solvent-induced fluorescence changes are characteristic of an excited state charge transfer (CT) in a polar solvent.<sup>1c,15a,16b,c</sup> The CT most likely occurs between the electron-donor dimethylamino group and the electron-acceptor boronic acid group. The  $sp^2$ -hybridized boron atom of the boronic acid group linked directly to the naphthalene can form a conjugated system with naphthalene and act as an electron-acceptor group because of the empty p orbital in the boron atom. Incorporation of a donor dimethylamino group on the same chromophore results in excited state CT and the emission appears at a longer wavelength (513 nm for compound **1**). Additionally, the sugar-induced emission changes of **1** can also be explained through a CT mechanism. Addition of a sugar lowers the  $pK_a$  of the boronic acid group and converts the neutral  $sp^2$  hybridization to the anionic  $sp^3$  hybridization. In the  $sp^3$  state, boronic acid can no longer act as an electron-acceptor group. As a result, the CT process is turned off and the emission appears at a shorter wavelength (433 nm). The fact that the  $\lambda_{\text{em}}$  for **1** is the

same in hexanes as it is in the presence of a sugar in phosphate buffer is also consistent with the disappearance of CT, both in hexanes and in the presence of a sugar in phosphate buffer.

To summarize, **1** shows significant ratiometric sensing properties upon binding with a sugar. Ratiometric fluorescent carbohydrate sensors, which have two or more emission maxima showing opposite changes in fluorescence emission in response to changes in carbohydrate concentrations, are potentially very useful. For example, ratiometric measurements can reduce or eliminate distortions of data caused by photo-bleaching, sensor concentration, illumination stability, *etc.*<sup>15</sup> However, ratiometric fluorescent carbohydrate sensors are rare<sup>16</sup> and compound **1** should become very useful in this role.

**Fluorescence properties of 4-DMANBA (2).** The sugar-induced fluorescence changes of **2** were studied in ways similar to those of 5-DMANBA (**1**). Although these two sensors are position isomers, they exhibit significantly different fluorescence properties. In 0.1 M aqueous phosphate buffer solution (pH 7.4), **2** exhibits emission [Fig. 11(A)] and absorption [Fig. 11(B)] maxima at 450 and 300 nm, respectively. The emission spectral changes of **2** with the addition of different sugars, that is, fructose, sorbitol, tagatose, galactose and glucose, were studied.<sup>11</sup> Significant fluorescence intensity changes were observed upon addition of sugar. For example, a 41-fold fluorescence intensity increase was observed after addition of 50 mM fructose. However, these changes occurred only at one

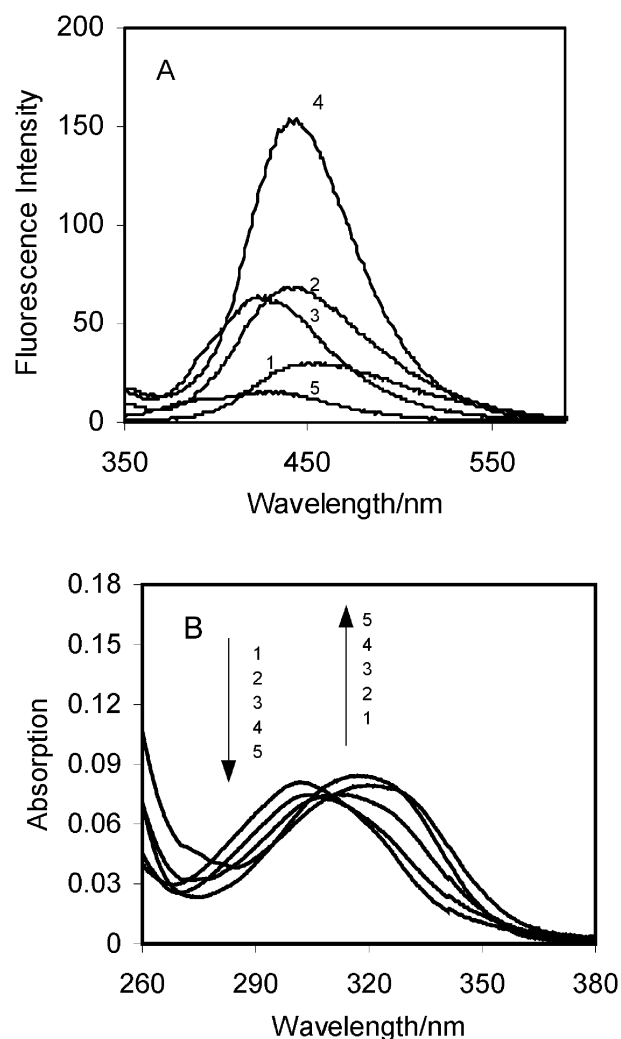


**Fig. 11** Emission (A) and absorption (B) spectra of **2** ( $1.0 \times 10^{-5}$  M) in 0.1 M aqueous phosphate buffer at pH 7.4 in different solvents: (curve 1) buffer; (curve 2) MeOH-buffer (1:1, v/v); (curve 3) MeOH; (curve 4) EtOAc; (curve 5) hexanes.

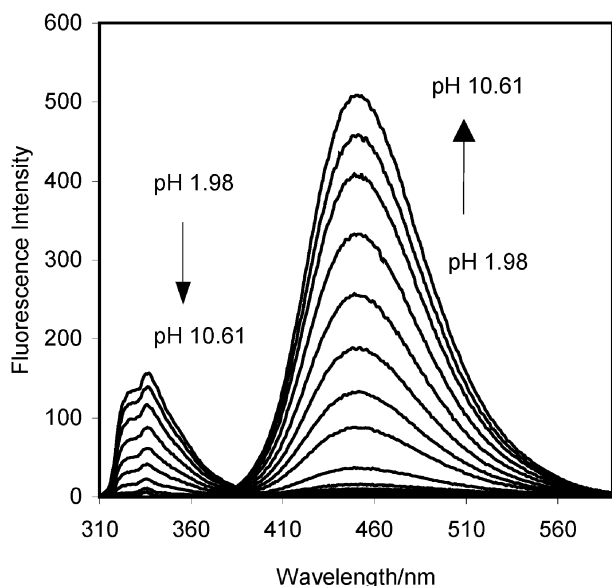


**Fig. 12** Fluorescence spectral changes of **2** ( $5.0 \times 10^{-6}$  M) in the absence of sugar at different pH, in 0.1 M aqueous phosphate buffer,  $\lambda_{\text{ex}} = 300$  nm.

wavelength and no ratiometric changes were observed, which is in direct contrast to what was observed with **1**. The association constants ( $K_a$ ) between **2** and these five carbohydrates are similar to those of **1** and the affinity trend for **2** follows that for **1** in the order sorbitol ( $K_a = 226 \text{ M}^{-1}$ ) > fructose ( $K_a = 207 \text{ M}^{-1}$ ) > tagatose ( $K_a = 116 \text{ M}^{-1}$ ) > galactose ( $K_a = 12 \text{ M}^{-1}$ ) > glucose ( $K_a = 4.0 \text{ M}^{-1}$ ).<sup>11</sup>

To establish what structural features led to the fluorescence intensity changes, we also studied the pH-induced fluorescence spectral changes of **2** in the absence of sugar and in the presence of fructose or glucose at a fixed concentration of 50 mM (Figs. 12 and 13). Fig. 12 shows the fluorescence spectral changes of **2** in the absence of sugar in the pH range 1.98–10.61. With increasing pH, the emission intensity of **2** at 336 nm decreases drastically, which corresponds to the change from the protonated form **2a** to the neutral form **2**, as depicted in Scheme 3. The emission intensity of **2**, in the absence of carbohydrate, increased by over 170-fold at 445 nm when the pH increased from 2 to 11. This fluorescence change trend is different from that of **1**, where only unidirectional changes were observed. This also means that the neutral species **2** is essentially nonfluorescent, and that only **2a** and **2b** are fluor-

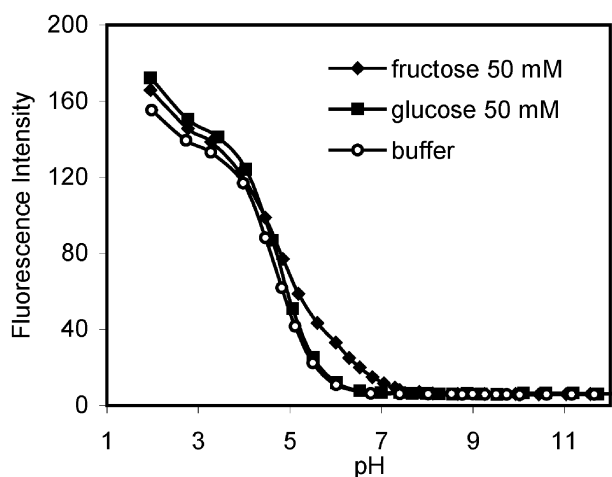
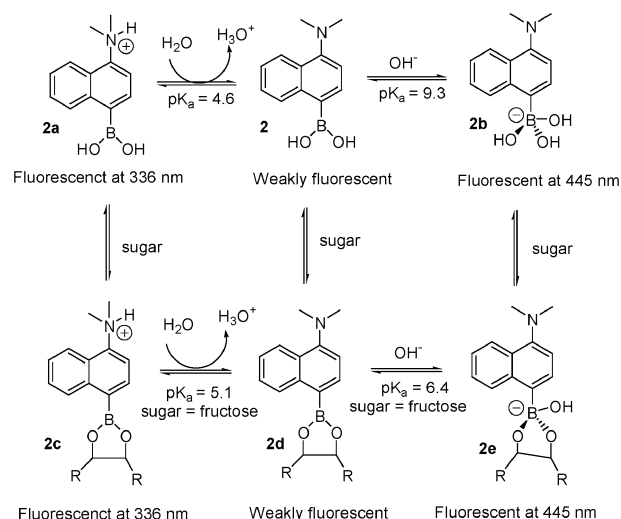


**Fig. 13** pH-dependent fluorescence intensity changes of **2** ( $5.0 \times 10^{-6}$  M) at 336 nm in the absence and in the presence of sugar in 0.1 M aqueous phosphate buffer,  $\lambda_{\text{ex}} = 300$  nm.



**Scheme 3** Fluorescence properties of **2** in different ionization states in the absence and in the presence of sugar in 0.1 M aqueous phosphate buffer.

escent, with emission maxima at 336 and 445 nm, respectively (Scheme 3).

The pH profiles of the fluorescence intensity of **2** at 336 nm in the absence of sugar and in the presence of fructose or glucose at a fixed concentration of 50 mM (Fig. 13) reveal that the  $pK_a$  of the aniline amino group remains the same, regardless of whether **2** is in the free form (**2a**) or complexed with a sugar (**2c**). The pH titration curves of **2** at 445 nm in the presence of fructose or glucose showed over 140-fold increases in fluorescence intensity when pH increased from 2 to 11.<sup>11</sup>

The fluorescence intensity changes of **2** at 445 nm in the absence and in the presence of a carbohydrate seem to correlate with the  $pK_a$  and hybridization change of the boron species upon going from the neutral trigonal form (**2**, **2d**) to the anionic tetrahedral form (**2b**, **2e**). In other words, the species that is responsible for the 445 nm emission is the tetrahedral anionic boronic acid (**2b**, **2e**). With the addition of **2** to **2e** that is responsible for the fluorescence intensity change at neutral pH.

Again, the difference in the pH titration curves is due to the difference in the apparent  $pK_a$  of the free sensor and its sugar complexes.<sup>11</sup> The pH profile of the solution in the presence of glucose also helps to explain why the maximum fluorescence intensity increase observed with physiological is not as high as that observed with fructose at physiological pH. The fructose complex has an apparent  $pK_a$  lower than 7. Therefore, at physiological pH (7.4), the complex exists entirely as the fluorescent species **2e**. However, for the glucose complex, the apparent  $pK_a$  is about 8.2, which means that only a fraction of the complex exists in the fluorescent form **2e** and a large percentage exists in the nonfluorescent neutral form **2d**. Therefore, the maximum fluorescence intensity for the glucose complex at pH 7.4 will only be a fraction of that of the fructose complex, assuming that they are equally fluorescent in the anionic form **2e**. This assumption is justified, since both the glucose and the fructose complexes give essentially the same fluorescence intensity at higher pH.

Similar to the analysis for **1**, the correlation of the different ionization states of **2** with its fluorescence property changes can be summarized as in Scheme 3. The protonated state (form **2a** and **2c**) is fluorescent at 336 nm, but nonfluorescent at 445 nm; the neutral state (form **2** and **2d**) is very weakly fluorescent at 450 nm and the anionic tetrahedral state (**2b** and **2e**) is fluorescent at 445 nm, but nonfluorescent at 336 nm. Compound **2** showed large, but non-ratiometric fluorescence changes upon addition of a sugar. These changes are consistent

with the conversion of the boron from the trigonal neutral form **2** to the anionic tetrahedral form **2e** upon carbohydrate addition, due to the decreased apparent  $pK_a$  of the complex (Scheme 3). Compound **2** can serve as an off-on fluorescent sensing system with excellent water solubility. The major difference between **1** and **2** in their fluorescence properties is that the neutral species is fluorescent for **1** (**1**, **1d**, Scheme 2), but nonfluorescent for **2** (**2**, **2d**, Scheme 3).

We have also studied the effect of solvent on the emission and absorption spectra of **2**. Only small wavelength changes were observed in both the emission and the absorption spectra of compound **2** (see Fig. 11). The emission wavelength changed from 450 nm in aqueous phosphate buffer to 425 nm in hexanes, while the absorption maximum changed from 300 nm in aqueous phosphate buffer to 317 nm in hexanes. These solvent-induced spectral changes in compound **2** suggested that excited state CT is not involved in the drastic fluorescence intensity changes observed upon addition of sugars.

## Conclusion

Two water-soluble naphthalene-based fluorescent saccharide sensor isomers, 5-(dimethylamino)naphthalene-1-boronic acid (5-DMANBA, **1**) and 4-(dimethylamino)naphthalene-1-boronic acid (4-DMANBA, **2**), have been synthesized and studied. The substitution pattern has a significant effect on the fluorescence property of these two compounds. **1** is a ratiometric sensor that shows large fluorescence intensity changes at two wavelengths, 513 and 433 nm, upon binding with a sugar at physiological pH. **2** is a useful water-soluble off-on fluorescent saccharide sensor that shows very large fluorescence intensity increases upon binding with a sugar at a single wavelength (445 nm). These fluorescent reporter compounds will be very useful for the construction of di- and multiboronic acid sensors (fluorescent boronolactins) for the highly specific identification and detection of biologically important carbohydrates.

## Experimental

### General

$^1\text{H}$  NMR spectra were recorded at 300 or 400 MHz and  $^{13}\text{C}$  NMR spectra at 75 or 100 MHz, with tetramethylsilane as the internal standard. Elemental analyses and mass spectral analyses were performed by the analytical and the mass spectrometry facilities of the Georgia State University. Fluorescence spectra were recorded on a Shimadzu RF-5301 PC spectrofluorometer. Absorption spectra were recorded on a Shimadzu UV-1700 UV-Visible spectrophotometer. All pH values were determined by a UB-10 Ultra Basic Benchtop pH meter (Denver Instrument). Column chromatography was performed on silica gel (200–400 mesh) from Aldrich. Tetrahydrofuran (THF) was distilled over Na before use.

### Synthesis

**5-Nitro-1-bromonaphthalene (4).**<sup>12a</sup> A mixture of 1-nitronaphthalene (**3**, 10.0 g, 58 mmol; mp 60 °C) and  $\text{FeCl}_3$  (0.066 g, 0.41 mmol) was heated to 90 °C. Then bromine (3.0 ml, 58 mmol) was added dropwise and the reaction mixture was stirred at 90 °C for 2 h. After cooling down to room temperature, the resulting crude material was recrystallized from ethanol to give **4** as yellow needle-shaped crystals (7.3 g, 50%); mp 119–120 °C.  $^1\text{H}$  NMR (300 MHz,  $\text{CDCl}_3$ )  $\delta$ : 8.44 (d,  $J$  = 8.7 Hz, 1H), 8.34 (d,  $J$  = 8.7 Hz, 1H), 8.13 (d,  $J$  = 7.5 Hz, 1H), 7.81 (d,  $J$  = 7.5 Hz, 1H), 7.56 (t,  $J$  = 8.1 Hz, 1H), 7.44 (t,  $J$  = 8.1 Hz, 1H);  $^{13}\text{C}$  NMR (75 MHz,  $\text{CDCl}_3$ )  $\delta$ : 147.2, 133.6, 132.7, 131.8, 129.6, 126.4, 125.7, 124.6, 123.7, 123.0; EI-MS ( $m/z$ ) calcd for  $\text{C}_{10}\text{H}_6\text{BrNO}_2$ : 251 ( $\text{M}^+$ ); found: 251.

**5-Amino-1-bromonaphthalene (5).**<sup>12b</sup> To a solution of **4** (2.5 g, 10 mmol) in EtOH–AcOH–dioxane– $\text{H}_2\text{O}$  (2:2:2:1, 30 ml) was added Fe (5.6 g, 100 mmol) and 2 drops of HCl (2 N). The reaction mixture was stirred at 100 °C for 2 h. After evaporation of the solvents, the residue was dissolved in 100 ml  $\text{CH}_2\text{Cl}_2$  and washed with 5%  $\text{NaHCO}_3$  (3  $\times$  30 ml) and dried over  $\text{Na}_2\text{SO}_4$ . After evaporation of the solvent, the crude mixture was chromatographed on a silica gel column, using  $\text{CH}_2\text{Cl}_2$ –hexanes (1:1) as the eluent, to give, after removal of the solvent, **5** as a white powder (3.0 g, 97%); mp 65–66 °C.  $^1\text{H}$  NMR (400 MHz,  $\text{CDCl}_3$ )  $\delta$ : 7.79 (d,  $J$  = 8.8 Hz, 1H), 7.76 (d,  $J$  = 8.0, 1H), 7.71 (d,  $J$  = 8.4 Hz, 1H), 7.39 (t,  $J$  = 7.6 Hz, 1H), 7.28 (t,  $J$  = 7.2 Hz, 1H), 6.83 (d,  $J$  = 7.2 Hz, 1H), 4.18 (s, 2H);  $^{13}\text{C}$  NMR (100 MHz,  $\text{CDCl}_3$ )  $\delta$ : 142.5, 133.0, 130.4, 128.0, 125.1, 125.0, 123.9, 121.0, 118.4, 110.9; ESI-MS ( $m/z$ ) calcd for  $\text{C}_{10}\text{H}_6\text{BrN}$  222.0 ( $\text{M} + \text{H}^+$ ); found 222.1. Anal. calcd for  $\text{C}_{10}\text{H}_6\text{BrN}$ : C, 54.08; H, 3.63; N, 6.31; found: C, 53.81; H, 3.46; N, 6.11.

**5-(Dimethylamino)-1-bromonaphthalene (6).**<sup>12b</sup> To a solution of **5** (0.8 g, 3.1 mmol) and  $\text{CH}_3\text{I}$  (1.9 ml, 31 mmol) in THF (50 ml) was added NaH (60%; 1.2 g, 31 mmol). The reaction mixture was stirred at 60 °C overnight. The precipitate was removed by filtration. After evaporation of the solvent, the residue was dissolved in 100 ml  $\text{CH}_2\text{Cl}_2$  and washed with 5%  $\text{NaHCO}_3$  (3  $\times$  30 ml) and dried over  $\text{Na}_2\text{SO}_4$ . After evaporation of the solvent, the crude product was chromatographed on a silica gel column, using  $\text{CH}_2\text{Cl}_2$ –hexanes (1:3) as the eluent, to give, after removal of the solvent, **6** as a colorless oil (0.66 g, 85%).  $^1\text{H}$  NMR (300 MHz,  $\text{CDCl}_3$ )  $\delta$ : 8.43 (d,  $J$  = 8.4 Hz, 1H), 8.06 (d,  $J$  = 8.4 Hz, 1H), 7.82 (d,  $J$  = 7.2, 1.2 Hz, 1H), 7.56 (t,  $J$  = 7.5, 0.9 Hz, 1H), 7.41 (t,  $J$  = 7.5, 0.9 Hz, 1H), 7.28 (d,  $J$  = 7.2, 2.4 Hz, 1H), 3.02 (s, 6H);  $^{13}\text{C}$  NMR (75 MHz,  $\text{CDCl}_3$ )  $\delta$ : 151.5, 133.5, 130.5, 130.2, 127.5, 125.6, 124.5, 123.5, 122.1, 115.2, 45.7; ESI-MS ( $m/z$ ) calcd for  $\text{C}_{12}\text{H}_{13}\text{BrN}$ : 250.0 ( $\text{M} + \text{H}^+$ ); found: 250.1.

**5-(Dimethylamino)-naphthalene-1-boronic acid (1).** A solution of **6** (0.38 g, 1.5 mmol) in THF (5 ml) was cooled to –78 °C. To the solution was added dropwise *n*-BuLi in hexanes (1.5 M; 1.4 ml, 2.1 mmol). The reaction mixture was stirred at –78 °C for 45 min and then  $(\text{MeO})_3\text{B}$  (0.57 ml, 5.1 mmol) was added. After stirring at –78 °C for 1 h, the temperature was warmed to room temperature and stirring was continued overnight. The solvent was removed in vacuum. The residue was dissolved in 100 ml  $\text{CH}_2\text{Cl}_2$  and washed with 5%  $\text{NaHCO}_3$  (3  $\times$  30 ml) and dried over  $\text{Na}_2\text{SO}_4$ . After evaporation of the solvent, the crude mixture was chromatographed on a silica gel column, using  $\text{CH}_2\text{Cl}_2$ –MeOH (20:1) as the eluent, to give, after removal of the solvent, **1** as a white powder (0.21 g, 65%), mp 95–96 °C.  $^1\text{H}$  NMR (300 MHz,  $\text{CD}_3\text{OD}$ )  $\delta$ : 8.25 (d,  $J$  = 9.6, 1H), 7.48–7.43 (m, 3H), 7.38 (t,  $J$  = 8.4, 1H), 7.09 (d,  $J$  = 8.1, 0.6 Hz, 1H), 2.94 (s, 6H);  $^{13}\text{C}$  NMR (75 MHz,  $\text{CD}_3\text{OD}$ )  $\delta$ : 151.4, 136.5, 129.8, 128.6, 125.9, 124.7, 124.4, 123.2, 113.9 44.58; HR-ESI-MS ( $m/z$ ) calcd for  $\text{C}_{12}\text{H}_{15}\text{BNO}_2$ : 216.1196 ( $\text{M} + \text{H}^+$ ); found: 216.1196.

### Procedure for sugar-binding studies

Distinct solutions of the sensors ( $2.0 \times 10^{-5}$  or  $1.0 \times 10^{-5}$  M) and the sugars (various concentrations) were prepared in 0.1 M phosphate buffer at pH 7.40. Then, 2 ml of a sensor solution was mixed with 2 ml of a sugar solution and, after stirring for 20 min, the mixture was transferred into a 1 cm quartz cell and the fluorescence intensity was recorded immediately.

### Acknowledgements

Financial support from the National Institutes of Health (CA88343 and NO1-CO-27184), the Georgia Cancer Coalition

through a Distinguished Cancer Scientist Award, and the Georgia Research Alliance through an Eminent Scholar endowment is gratefully acknowledged.

## References

- For reviews, see: (a) W. Wang, X. Gao and B. Wang, *Curr. Org. Chem.*, 2002, **6**, 1285; (b) T. D. James, P. Linnane and S. Shinkai, *Chem. Commun.*, 1996, 281; (c) A. P. de Silva, H. Q. N. Gunaratne, T. Gunnlaugsson, A. J. M. Huxley, C. P. McCoy, J. T. Rademacher and T. E. Rice, *Chem. Rev.*, 1997, **97**, 1515; (d) J. H. Hartley, T. D. James and C. J. Ward, *J. Chem. Soc., Perkin Trans. 1*, 2000, 3155; (e) W. Yang, X. Gao and B. Wang, *Med. Res. Rev.*, 2003, **23**, 346; (f) S. Striegler, *Curr. Org. Chem.*, 2003, **7**, 81.
- (a) J. Yoon and A. W. Czarnik, *J. Am. Chem. Soc.*, 1992, **114**, 5874; (b) T. D. James, K. R. A. S. Sandanayake and S. Shinkai, *J. Chem. Soc., Chem. Commun.*, 1994, 477; (c) H. Eggert, J. Frederiksen, C. Morin and J. C. Norrild, *J. Org. Chem.*, 1999, **64**, 3846; (d) W. Yang, H. He and D. G. Drueckhammer, *Angew. Chem., Int. Ed.*, 2001, **40**, 1714; (e) H. Cao, D. I. Diaz, N. DiCesare, J. R. Lakowicz and M. D. Heagy, *Org. Lett.*, 2002, **4**, 1503; (f) N. DiCesare and J. R. Lakowicz, *Anal. Biochem.*, 2001, **294**, 154; (g) C. J. Ward, P. Patel, P. R. Ashton and T. D. James, *Chem. Commun.*, 2000, 229; (h) V. L. Alexeev, A. C. Sharma, A. V. Goponenko, S. Das, I. K. Lednev, C. S. Wilcox, D. N. Finegold and S. A. Asher, *Anal. Chem.*, 2003, **75**, 2316; (i) P. R. Westmark, S. J. Gardiner and B. D. Smith, *J. Am. Chem. Soc.*, 1996, **118**, 11093; (j) S. P. Draffin, P. J. Duggan and S. A. M. Duggan, *Org. Lett.*, 2001, **3**, 917; (k) J. J. Lavigne and E. V. Anslyn, *Angew. Chem., Int. Ed.*, 1999, **38**, 3666; (l) D. Stones, S. Manku, X. Lu and D. G. Hall, *Chem.-Eur. J.*, 2004, **10**, 92–100; (m) A. M. Irving, C. M. Vogels, L. G. Nikolcheva, J. P. Edwards, X. F. He, M. G. Hamilton, M. O. Baerlocher, F. J. Baerlocher, A. Decken and S. A. Westcott, *New J. Chem.*, 2003, **27**, 1419; (n) H. R. Mulla, N. J. Agard and A. Basu, *Bioorg. Med. Chem. Lett.*, 2004, **14**, 25; (o) V. R. R. Karnati, X. Gao, S. Gao, W. Yang, W. Ni and B. Wang, *Bioorg. Med. Chem. Lett.*, 2002, **12**, 3373.
- (a) J. M. Sugihara and C. M. Bowman, *J. Am. Chem. Soc.*, 1958, **80**, 2443; (b) J. P. Lorand and J. O. Edwards, *J. Org. Chem.*, 1959, **24**, 769; (c) G. Springsteen and B. Wang, *Tetrahedron*, 2002, **58**, 5291; (d) J. Yan, G. Spingsteen, S. Deeter and B. Wang, *Tetrahedron*, 2004, **60**, 11205.
- (a) W. Yang, S. Gao, X. Gao, V. R. R. Karnati, W. Ni, B. Wang, W. B. Hooks, J. Carson and B. Weston, *Bioorg. Med. Chem. Lett.*, 2002, **12**, 2175; (b) W. Yang, H. Fan, X. Gao, S. Gao, V. R. R. Karnati, W. Ni, W. B. Hooks, J. Carson, B. Weston and B. Wang, *Chem. Biol.*, 2004, **11**, 439; (c) T. J. Burnett, H. C. Peebles and J. H. Hageman, *Biochem. Biophys. Res. Commun.*, 1980, **96**, 157.
- (a) R. M. Bill, L. Revers and I. B. H. Wilson, *Protein Glycosylation*, Kluwer Academic Publishers, Boston, 1998; (b) A. Varki, R. Cummings, J. Esko, H. Freeze, G. Hart and J. Marth, *Essentials of Glycobiology*, Cold Spring Harbor Laboratory Press, Cold Spring Harbor, NY, 1999; (c) E. Sivridis, A. Giatromanolaki, M. Koukourakis and N. Agnantis, *Virchows Arch.*, 2000, **436**, 52; (d) M. Schwarz, L. Spector, A. Gargir, A. Shtevi, M. Gortler, R. T. Altstock, A. A. Dukler and N. Dotan, *Glycobiology*, 2003, **13**, 749.
- For reviews, see: (a) T. Feizi, *Curr. Opin. Struct. Biol.*, 1993, **3**, 701; (b) P. Sears and C.-H. Wong, *Angew. Chem., Int. Ed.*, 1999, **38**, 2301; (c) S. Striegler, *Curr. Org. Chem.*, 2003, **7**, 81; (d) S. G. Turville, P. U. Cameron, D. Hart and A. L. Cunningham, *Trends Glycosci. Glycotechnol.*, 2002, **14**, 255; (e) C.-L. Schengrund, *Biochem. Pharmacol.*, 2003, **65**, 699.
- (a) M. Fukuda, *Cell Surface Carbohydrates and Cell Development*, CRC Publisher, Boca Raton, FL, 1992; (b) G. Ragupathi, *Cancer Immunol. Immun.*, 1996, **43**, 152; (c) G. Ragupathi and P. O. Livingston, *Recent Res. Develop. Cancer*, 2000, **2**, 39; (d) R. S. Haltiwanger and J. B. Lowe, *Annu. Rev. Biochem.*, 2004, **73**, 491; (e) T. Jorgensen, A. Berner, O. Kaalhus, K. J. Tveter, H. E. Danielsen and M. Bryne, *Cancer Res.*, 1995, **55**, 1817; (f) H. A. Idikio, *Glycoconjugate J.*, 1997, **14**, 875.
- (a) E. Liener, N. Sharon and I. J. Goldstein, *The Lectins: Properties, Functions, and Applications in Biology and Medicine*, Academic Press, Orlando, FL, 1986; (b) H.-J. Gabius and S. Gabius, *Lectins and Glycobiology*, Springer-Verlag, Berlin, New York, 1993.
- W. Yang, X. Gao and B. Wang, in *Organoboronic Acids*, ed. D. Hall, Wiley-VCH, 2004, pp. 481–512.
- W. Yang, L. Lin and B. Wang, *Heterocycl. Commun.*, 2004, **10**, 383.
- X. Gao, Y. Zhang and B. Wang, *Org. Lett.*, 2003, **5**, 4615.
- (a) C. C. Price and S.-T. Voong, *J. Org. Chem.*, 1949, **14**, 111; (b) L. Horner and J. Mathias, *J. Organomet. Chem.*, 1985, **282**, 175.
- M. Goldman and E. L. Wehry, *Anal. Chem.*, 1970, **42**, 1186.
- (a) S. Hamai, *Bull. Chem. Soc. Jpn.*, 1982, **55**, 2721; (b) F. G. Sanchez, M. H. Lopez and J. C. M. Gomez, *Analyst*, 1987, **112**, 1037; (c) L. Tong, *Cyclodextrin Chemistry—Base and Applications*, Scientific Press, Beijing, China, 2001, p. 145; (d) S. Fery-Forgues, M. T. Le Bris, J.-P. Guetté and B. Valeur, *J. Phys. Chem.*, 1988, **92**, 6233.
- (a) J. R. Lakowicz, *Principles of Fluorescence Spectroscopy*, Plenum Press, New York, 2nd edn., 1999; (b) G. Grynkiewicz, M. Poenie and R. Y. Tsien, *J. Biol. Chem.*, 1985, **260**, 3440.
- (a) A. P. Russell, *US Pat.* 5,137,833, 1992; (b) N. DiCesare and J. R. Lakowicz, *J. Phys. Chem. A*, 2001, **105**, 6834; (c) N. DiCesare and J. R. Lakowicz, *J. Photochem. Photobiol.*, 2001, **143**, 39; (d) S. Arimori, L. I. Bosch, C. J. Ward and T. D. James, *Tetrahedron Lett.*, 2001, **42**, 4553.